

Soft Matter Technology at KIT: Chemical Perspective from Nanoarchitectures to Microstructures

Sylvain Grosjean, Mirella Wawryszyn, Hatice Mutlu, Stefan Bräse, Joerg Lahann, and Patrick Theato*

Bioinspiration has emerged as an important design principle in the rapidly growing field of materials science and especially its subarea, soft matter science. For example, biological cells form hierarchically organized tissues that not only are optimized and designed for durability, but also have to adapt to their external environment, undergo self-repair, and perform many highly complex functions. Being able to create artificial soft materials that mimic those highly complex functions will enable future materials applications. Herein, soft matter technologies that are used to realize bioinspired material structures are described, and potential pathways to integrate these into a comprehensive soft matter research environment are addressed. Solutions become available because soft matter technologies are benefitting from the synergies between organic synthesis, polymer chemistry, and materials science.

1. Introduction

Historically, mankind has made use of materials readily available from nature. In this century, however, there has

been a significant trend to prepare novel materials to meet increasingly complex and demanding requirements, an ability that often depends on the latest in scientific knowledge.^[1] Tight integration of interdisciplinary science is paving the way for advancements in fundamental and applied science by particularly focusing on the interface between divergent fields such as organic synthesis, polymer chemistry, and materials science among others, and hence, implementing new materials at near molecular scale precision in ways that are not even found in nature.^[2,3] Furthermore, by virtue of bioinspired (i.e., biomimetic)^[4–6] design strategies, it is an ongoing aim to

improve and disrupt the development of man-made materials toward state-of-the-art matter ranging from nanoarchitectures to microstructures.^[7]

Hitherto, by virtue of bioinspired approaches (such as bioadhesion and self-assembly), we were able to fabricate soft materials with tailor-specific properties (e.g., sophisticated structures, hierarchical organizations, controlled selectivity, or anti-fouling) by adopting various synthetic chemistry approaches in order to change the polymers' physical properties—as Pierre-Gilles de Gennes depicted a typical feature of soft matter “is the fact that a very mild chemical action [can induce] a drastic change in mechanical properties”.

In this spirit, synthetic approaches enable features such as stimuli response which in turn allow for polymers to (ir-)reversibly change their mechanical properties, for instance, stiffness, shape, or porosity. Consequent mechanical morphing effects of artificial materials can be utilized in turn to mimic nature, thereby, adapting concepts to control systems from the nano- to macroscale range.

Unlike many “conventional” international, multidisciplinary “soft matter” research groups world-wide,^[8] the “Soft Matter Synthesis Laboratory (SML)” at Karlsruhe Institute of Technology (KIT) founded in 2011 is a synthetic platform of the BioInterfaces Technology and Medicine Programme, with its long-term research mission to develop technologies enabling the design of soft materials with unprecedented properties emerging on the interface between organic synthesis, polymer chemistry, and materials science, and hence to address grand social and scientific challenges. Complex technologies call for knowledge and skills that may cut across several disciplines, with an increasing need for cross-, multi-, inter-, and

Dr. S. Grosjean, Dr. M. Wawryszyn, Dr. H. Mutlu, Prof. S. Bräse, Prof. J. Lahann, Prof. P. Theato
Soft Matter Synthesis Laboratory
Institute for Biological Interfaces 3 (IBG 3)
Karlsruhe Institute of Technology (KIT)
Hermann-von-Helmholtz-Platz 1
76344 Eggenstein-Leopoldshafen, Germany
E-mail: patrick.theato@kit.edu

Dr. S. Grosjean, Dr. M. Wawryszyn, Dr. H. Mutlu, Prof. S. Bräse, Prof. J. Lahann, Prof. P. Theato
Institute for Toxicology and Genetics (ITG)
Karlsruhe Institute of Technology (KIT)
Hermann-von-Helmholtz-Platz 1
76344 Eggenstein-Leopoldshafen, Germany

Dr. S. Grosjean, Dr. M. Wawryszyn, Dr. H. Mutlu, Prof. S. Bräse, Prof. J. Lahann, Prof. P. Theato
Institute for Functional Interfaces (IFG)
Karlsruhe Institute of Technology (KIT)
Hermann-von-Helmholtz-Platz 1
76344 Eggenstein-Leopoldshafen, Germany

 The ORCID identification number(s) for the author(s) of this article can be found under <https://doi.org/10.1002/adma.201806334>.

© 2019 The Authors. Published by WILEY-VCH Verlag GmbH & Co. KGaA, Weinheim. This is an open access article under the terms of the Creative Commons Attribution-NonCommercial-NoDerivs License, which permits use and distribution in any medium, provided the original work is properly cited, the use is non-commercial and no modifications or adaptations are made.

DOI: 10.1002/adma.201806334

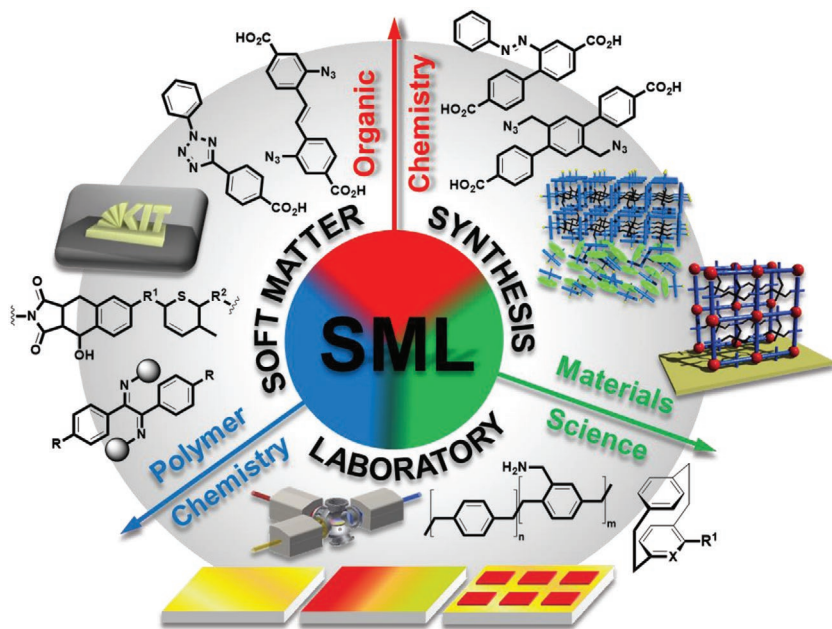


Figure 1. Overview of the Soft Matter Synthesis Laboratory activities and research fields. The image of the 3D model of the KIT logo is adapted with permission.^[32] Copyright 2018, Wiley-VCH.

transdisciplinary approaches, and the SML at KIT provides such a unique platform to master future synthetic challenges. The very core of materials science, the relation of properties to structure and composition, implies a need for the combined efforts of basic fundamental research fields such as pure organic synthesis and polymer chemistry (see **Figure 1** and also Table S1 in the Supporting Information). As such, the SML at KIT focuses on functional nanoarchitectures in 1D, 2D, and 3D.

In the following sections, we aim to demonstrate how advanced materials are emerging through the collaborations in SML between transdisciplinary fields among international members. Note, we also emphasize that here we in no way cover all the research activities conducted at the SML but focus rather on recent interdisciplinary examples.

2. Research Activities in SML

Bioinspired approaches such as bioadhesion or self-assembly motivate for the fabrication of soft materials with specifically tailored properties (e.g., sophisticated structures, hierarchical organizations, controlled selectivity, or antifouling) by adopting various stimuli including enzymes, light, or temperature and by utilization of responsive smart chemistries (Diels–Alder [4 + 2] cycloaddition reaction,^[9] nitrile imine-mediated tetrazole–ene cycloaddition (NITEC),^[10] and photo-triggered oxime ligation).^[11–13] Indeed, the use of light to control the course of a (bio)chemical reaction is an attractive idea due to its ease of establishing high precision and fine spatial resolution.^[14] For instance, relevant to the area of bioadhesion, numerous examples of rare and exciting phenomena have been reported.^[15–17] Particularly, a photoconjugation strategy based

on light-triggered Diels–Alder addition of *o*-quinodimethanes is compatible with biomolecules and proceeds rapidly at ambient temperature without the need of a catalyst.^[15] The spatial control is confirmed by photopatterning of a small-molecule atom-transfer radical polymerization (ATRP) initiator, a polymer, and a peptide in a time-of-flight secondary-ion mass spectrometry investigation. Respective bioinspired poly(dopamine) (PDA) films were equipped with antifouling poly[monomethoxy oligo(ethylene glycol) methacrylate], poly(MeOEGMA), brushes utilizing an NITEC-based phototriggered surface encoding protocol. The antifouling brushes were photopatterned on PDA surfaces, leading cells to form confluent layers in the nonirradiated sections, while no adhesion occurred on the brushes resulting in a remarkably precise cell pattern. The presented strategy paved the way for the design of tailor-made patterned cell interfaces.

Concomitantly, the NITEC reaction has also been successfully employed in polymer ligation,^[18] protein and peptide functionalization,^[19] to trigger photoswitchable wettability,^[20] redox and radical sensor formation,^[21] self-reporting fluorescent polymers,^[22] the preparation of degradable fluorescent single-chain^[23] nanoparticles and networks.^[24] Specifically, the latter aimed for the adoption of a fluorescence-based methodology enabling the quantification of ligation points in photochemically prepared polymer networks. To accomplish this, well-defined α,ω -tetrazole-capped polymer strands were prepared via reversible addition-fragmentation chain transfer (RAFT) polymerization and further cross-linked under UV irradiation by a trimaleimide via NITEC. At each linkage point, it is assumed that a fluorescent pyrazoline ring is formed, hence resulting in fluorescent networks, which are degradable by aminolysis of the trithiocarbonate functionalities, leading to soluble fragments. The fluorescence emission of the soluble network fragments correlated directly with the number of pyrazoline moieties originally present in the network. In this way, a direct measure of the number of ligation points constituting the network is accomplished (**Figure 2a**).

Furthermore, nitroxide-functionalized surfaces using a bioinspired adhesion technique were engineered (**Figure 2b**).^[25] Hence, a versatile surface modification strategy based on mussel-inspired oxidative catecholamine polymerization was adopted for the design of a nitroxide-containing thin polymer film poly[(3,4-dihydroxy-*l*-phenylalanine)-(2,2,6,6-tetramethylpiperidine-1-oxyl)], poly(DOPA-TEMPO). Successfully, various types of substrates including silicon, titanium, ceramic alumina, and poly(tetrafluoroethylene) were coated with poly(DOPA-TEMPO) films in a one-step dip-coating procedure under aerobic, slightly alkaline (pH 8.5) conditions. The heterogeneous composition of surface-adherent nitroxide scaffolds examined by X-ray photoelectron spectroscopy was correlated to that examined by in-solution polymer analysis via high-resolution electrospray ionization mass spectrometry, revealing oligomeric structures with up to six

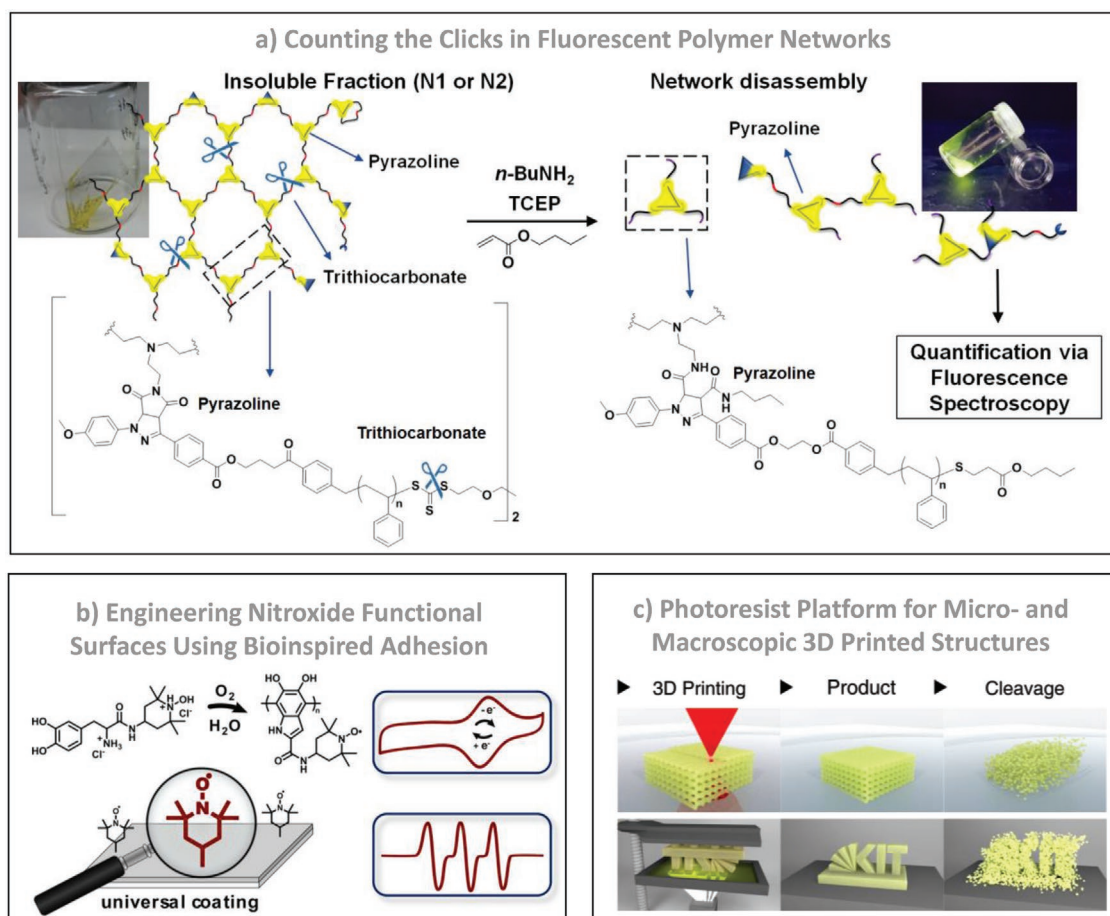


Figure 2. a) A facile and powerful methodology to estimate the amount of cross-linking points in networks via fluorescence spectroscopy, exploiting the self-reporting properties of NITEC. Adapted with permission.^[24] Copyright 2018, Wiley-VCH. b) A design of a nitroxide-containing polymer scaffold equipped with mussel-like adhesive properties for the facile coating and substrate-independent decoration of various materials with nitroxides. Adapted with permission.^[25] Copyright 2018, American Chemical Society. c) Introducing a simple and subtractive photoresist, resting on commercially available components with a formulation requiring minimal preparation time. Adapted with permission.^[32] Copyright 2018, Wiley-VCH.

repeating units, mainly composed of covalently linked dihydroxyindole along the polymer backbone. Relevant to the nitroxide chemistry, we also showed that the nitroxide-containing macromolecules possessing side-chain unpaired electrons delocalized over the N–O bond exhibit wide applicability as self-reporting systems based on the nitroxide-induced fluorescence quenching.^[26] In addition, we pioneered the formation of self-reporting and refoldable profluorescent single-chain nanoparticles via the light-induced reaction ($\lambda_{\text{max}} = 320 \text{ nm}$) of nitroxide radicals with a novel bifunctional cross-linker bearing a photoreactive functionality (Irgacure 2959).^[27]

Materials science often requires smart materials (stimuli-responsive materials)^[28] with unique properties, i.e., materials capable of changing their properties in a controlled way in response to external triggers.^[29,30] Sophisticated techniques, developed within the recent decades, opened the doors to creative and novel possibilities. For instance, manufacturing has been revolutionized by advances in 3D printing,^[31] as well as entirely new methods for creating complex structures from unfolding or stretching of patterned 2D composites. Particularly, selective removal of structural elements

plays a decisive role in 3D printing applications enabling complex geometries (Figure 2c).^[32] Smart materials found immense applications, often inter alia with the development of stimuli-responsive polymers, which has been highlighted in several reviews,^[33,34] including those found in the area of soft robotics.^[35,36]

Combining organic synthesis with engineering aspects in a multidisciplinary mindset led in our case to the implementation of tailor-made organic structures by chemical vapor deposition (CVD) or electro-hydrodynamic cojetting (EHD) techniques. For example, CVD-coated polymer films with versatile surface functions or electrojetted micro- to nanoparticles with stimuli-responsive functions find already day-to-day usage in industry and biomedicine.^[37] Thus, fast and easy approaches to gain specifically shaped or coated smart materials rendered by the above-mentioned techniques are highlighted (Figure 3).

CVD polymerization of poly(*p*-xylylene) (PPX) led to a new and unconventional class of smart materials, ever since the gas-phase pyrolysis of these cyclic dimers was reported by Brown and Farthing.^[38] Stable ultrathin film coatings are formed through homolytically cleavage of the [2.2]paracyclophane's

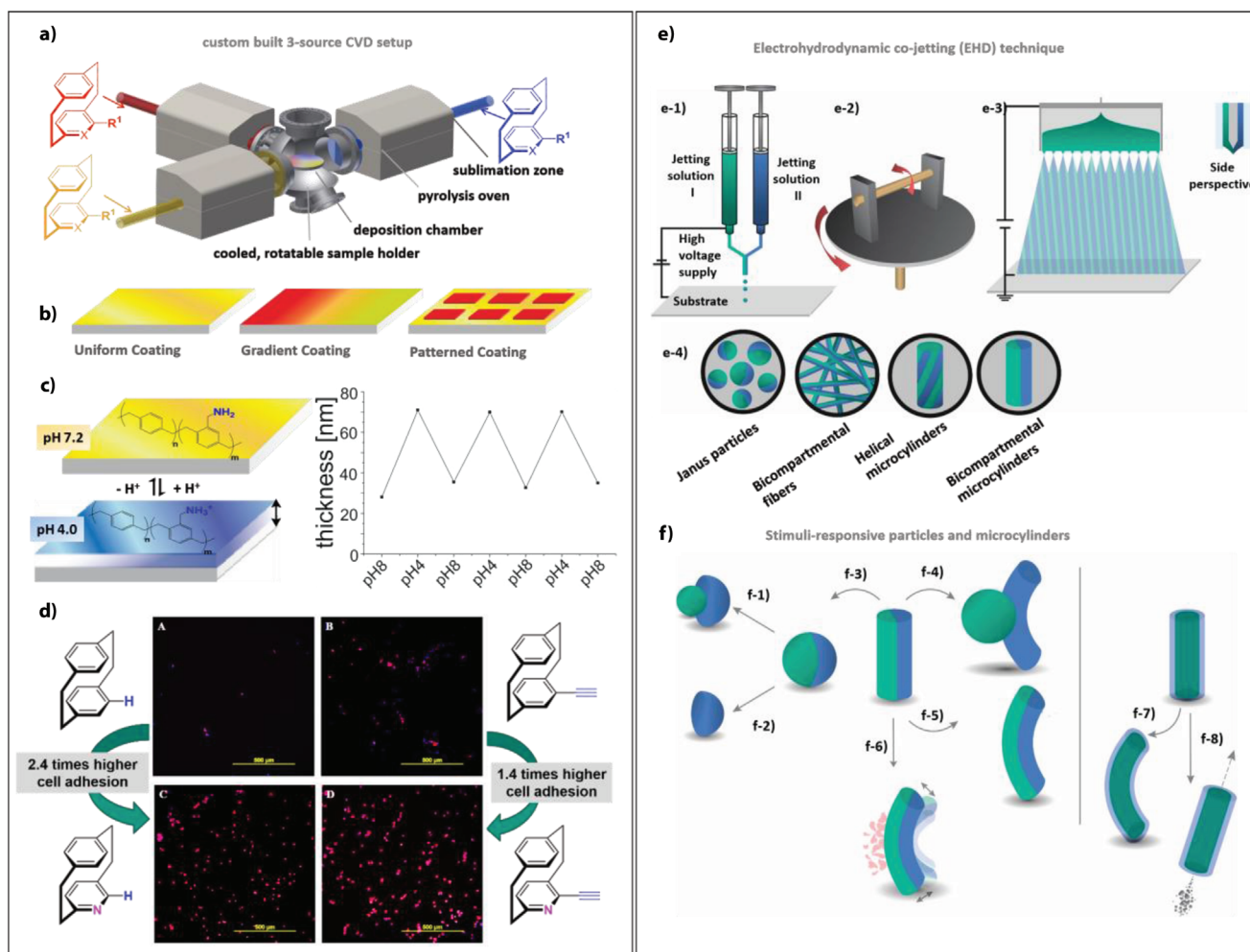


Figure 3. a) Multisource chemical vapor deposition (CVD) setup to form stable poly(*p*-xylylene) (PPX) based ultrathin films on surfaces. b) Specific examples of surface structuring of PPX-based coatings. c) pH-responsive functionalized PPX-coatings: pH-dependent swelling is measured by spectroscopic ellipsometry. d) PPX-backbone modification by incorporation of nitrogen heteroatoms increases endothelial cell adhesion. e) Electro-hydrodynamic (EHD) co-jetting process to create micro- to nanoparticles and microcylinders. e-1) Dual capillary needle system used for EHD co-jetting—the system can be extended up to seven side-by-side capillaries. e-2) The twisting motion of two threads actuated by two oppositely directed rotary axes leading to helical fibers. e-3) Extended fluid interface system enabling a needleless EHD process. e-4) Examples of different EHD techniques. f) Examples for stimuli-responsive particles and microcylinders triggered by external factors. f-1) Cartoon of a particle with two distinct compartments produced by EHD co-jetting, with one compartment made of a pH-responsive polymer that swells with changes in pH. f-2) Particle degradation as a response to UV light in addition to an oxidizing agent. f-3) Shape-shifting bicompartamental microcylinder to spheres by ultrasound and usage of the same polymer for both compartments. f-4) Shape-shifting of bicompartamental microcylinder to a snail-like particle by ultrasound and different polymers for both compartments. f-5) Reversible three-way toggling bicompartamental microcylinder by the use of different compartments and solvents. f-6) Synchronized contraction of biohybrid microcylinders triggered by spontaneous contraction of the cardiomyocytes. f-7) Hollow microtubes with coaxial compartments can be used as microcontainers, where the shape-shifting is triggered by solvents with different polarities. f-8) Self-actuating biohybrid anisotropic microcylinders exerting gas bubbles. The schematic representation of the CVD setup in (a) is copyright of and reproduced with permission of C. Hussal, Logos Verlag, Berlin, Germany 2017. c) Adapted with permission.^[45] Copyright 2017, Wiley-VCH. d) Adapted with permission.^[46] Copyright 2017, Wiley-VCH. e-1) Adapted with permission.^[54b] Copyright 2013, Wiley-VCH. e-2) Adapted with permission.^[52] Copyright 2018, Wiley-VCH. e-3) Adapted with permission.^[51] Copyright 2016, Wiley-VCH. e-4) Adapted with permission.^[51] Copyright 2016, Wiley-VCH.

(PCP) ethylene bridges and subsequent polymerization. Synthetic variations of PCP led to a wide variety of (a)chiral PCP derivatives enabling the CVD process of phane-based structures, suitable for (opto)electronics and biomedical devices.^[39,40] A great advantage of the CVD process regarding PCP derivatives is the ability of substrate-independent coating and the avoidance of solvents or catalysts (Figure 3a).^[41] Alternative approaches leading to PPX surfaces, such as initiated and oxidative chemical vapor deposition (iCVD and oCVD) or the

Gilch process, are described elsewhere.^[42,43] Advantageously, structuring techniques, such as homopolymer, copolymer, uniform, gradient or patterned coatings, enable the design of surfaces with tailor-made functions and properties (Figure 3b).^[44]

For example, a stimuli-responsive PPX-based coating bearing methylamine moieties leads to ionizable amino groups, resulting in pH-dependent swelling behavior and subsequent thickness increase.^[45] Decreasing the pH from 8 to 4 resulted in an increase of the surface thickness of 30 nm

(Figure 3c). Moreover, stimuli responsiveness is not restricted to specific side groups along the polymer chain but also to the chemical modification of the PPX backbone. Incorporation of a nitrogen atom into the aromatic system significantly increases the cell adhesion properties (Figure 3d). Pyridinophane-based coatings trigger primary human umbilical vein endothelial cells (HUVECs) to spread out approximately twice in comparison to HUVECs on nitrogen-free PPX coatings, due to a polarity increase of the poly(2,5-lutidinylene-co-p-xylylene) compared to PPX.^[46]

EHD also allows for preparation of sophisticated stimuli-responsive particles, such as dynamically reconfigurable or shape-memory microcylinders mimicking biological machineries. Triggered by external stimuli, spherical- or cylindrical-shaped colloids respond by swelling, degrading, shape-/size-/curvature-shifting, moving, or rhythmic bending behavior, thus, being candidates for controlled drug release, synthetic sensors, bioactuators, or even miniaturized biorobots. The design of well-shaped particles with a narrow size distribution has become possible by the particle fabrication in nonwetting templates (PRINT) technology, layer-by-layer (LbL) fabrication, or stop-flow lithography.^[47,48]

EHD was optimized for anisotropic particles and microcylinders by Lahann et al. (Figure 3e).^[49] Within the **EHD** process, electro-co-spinning of two or more polymeric solutions in laminar flow, convective mixing is minimized, and the particle's size is controlled by parameters such as the dielectric constant of the solvent or charge (Figure 3e-1).^[50] An alignment of the jetted fibers can be achieved by implying a secondary ring electrode.^[51] Moreover, helical bicompartamental fibers are manufacturable by in situ twisting of the two threads into opposite directions during co-electrospinning with a collector system containing two rotary axes (Figure 3e-2).^[52] Microtubular particles with a defined thickness from 10 to 200 μm are featured by cryosectioning of the jetted fibers.^[53] Multicompartamental side-by-side capillary needle systems allow for Janus- or multi-compartamental particles/microcylinders, whereas coaxially positioned needles with an outer and an inner needle feature core-shell particles or tubular microcylinders (Figure 3e-4). Noteworthy, needleless **EHD** process enables a 30 times higher throughput in comparison to conventional needle-based technique (Figure 3e-3).^[51]

EHD particles and cylinders compelled to a specific form or motion by environmental triggers are presented in the following (Figure 3f). As a drug-delivery system for personalized biomedical treatment, the release of appropriate siRNA serving as a gene-silencing drug against specific cancer cell lines (MDA-MB-231/GFP) has been achieved by employing bicompartamental poly(D/L-lactide-co-glycolic acid)/polyethyleneimine (PLGA/PEI) nanocarriers with an average size of 216 nm as delivery vectors for small interfering RNA (siRNA) (Figure 3f-1).^[50] The higher swelling capacity of the PEI compartment at lower pH ensures the endosomal escape of the siRNA by mechanically breaking or osmotic bursting of the endosome.

Controlled particle degradation can be considered as an alternative option for drug release. For example, multifunctional poly(ethylene glycol) (PEG)-based polymer particles comprising redox-responsive thioether moieties and light-sensitive o-nitrobenzyl (ONB) groups enable a cooperative interplay between photo- and redox response, resulting in a water-soluble

PEG compartment through sulfoxide formation of the thiol moieties and carboxylic acid formation by photocleavage of the hydrophobic ONB groups (Figure 3f-2).^[54a]

Shape-responsive architectures are an interesting class of materials for use soft robotics. PLGA microcylinders (70 μm long, 20 μm diameter) could be transformed irreversibly into spheres upon exposure to ultrasound, i.e., inducing a local heating above a T_g of 47–48 $^{\circ}\text{C}$ (Figure 3f-3).^[55] This approach can be extended by utilizing poly(methyl methacrylate)/poly(D/L-lactide-co-glycolic acid) (PMMA/PLGA) microcylinders, which transformed partially into snail-like particles, due to the higher T_g of PMMA (115–116 $^{\circ}\text{C}$), leaving the PMMA compartment unaffected (Figure 3f-4). Subtle playing with the polymers' surface tension by solvent variation allows for a reversible bending of poly(vinyl cinnamate) (PVCi)/(PEO/PEI) microcylinders. Reversible and highly repeatable particle expansion and retraction by continuous transition from a concave to a convex actuation angle (Figure 3f-5) can be used for reversible grabbing and releasing micrometer scale objects. Also, shape-shifting hollow microtubes, induced by ultrasound exposure, have been created on the basis of core/shell PEO/PLGA hollow microtubes with coaxial compartments (diameter = 17 μm , cavity = 6 μm), serving as microcontainers holding picoliters of pharmaceutical drugs for controlled release (Figure 3f-7).^[53] Microcylinders serving as microrockets have been prepared by electrospinning luminal microtubes and decoration with platinum nanoparticles, which trigger disproportionation of 10% H_2O_2 into propelling oxygen bubbles resulting in a spiral trajectory with a velocity of $100 \pm 20 \mu\text{m s}^{-1}$ (Figure 3f-8).^[53] Similarly, catalase as a biosource analog to platinum nanoparticles (PtNPs) catalyzes the disproportionation of H_2O_2 , while adhering on the inner tubular side. Further, motion induced by synchronized contraction of attached neonatal rat cardiomyocytes leading to rhythmic bending was demonstrated for PLGA-PEG/(PLGA/poly(lactide-co-caprolactone) (PLCL)) bicompartamental microcylinders (Figure 3f-6).^[56]

Another fascinating research area aims to control materials' structure and composition at the nanometer or even sub-nanometer scale to achieve unique properties and dedicated functionalities that do not exist in natural materials. In the last two decades, metal-organic frameworks (MOFs), also known as porous coordination polymers, have drawn the attention of both chemistry and materials community, as a new kind of porous material.^[57] By virtue of their 3D structure exhibiting huge porosity with record-breaking surface areas and pore volumes,^[58] MOFs were initially developed for applications in gas separation and storage.^[59] Later, MOFs have found more technologically advanced applications in catalysis,^[60] as sensors,^[61] containers for drug delivery,^[62] or membranes for separation or proton conductance. MOFs are formed by coordinating metal nodes and organic building blocks, referred to as organic linkers and are structurally flexible owing to many factors (e.g., the moderate metal-ligand interactions, the versatile configuration of metal ions/clusters, and the nature of the organic ligands). This extraordinary degree of variance in both the inorganic and organic components of their structures makes MOFs not only a highly flexible class of materials but also prime examples of the necessary interdisciplinary research at SML.

Consequently, the diversity of potential building blocks leads to an increasing demand for the design and synthesis of new

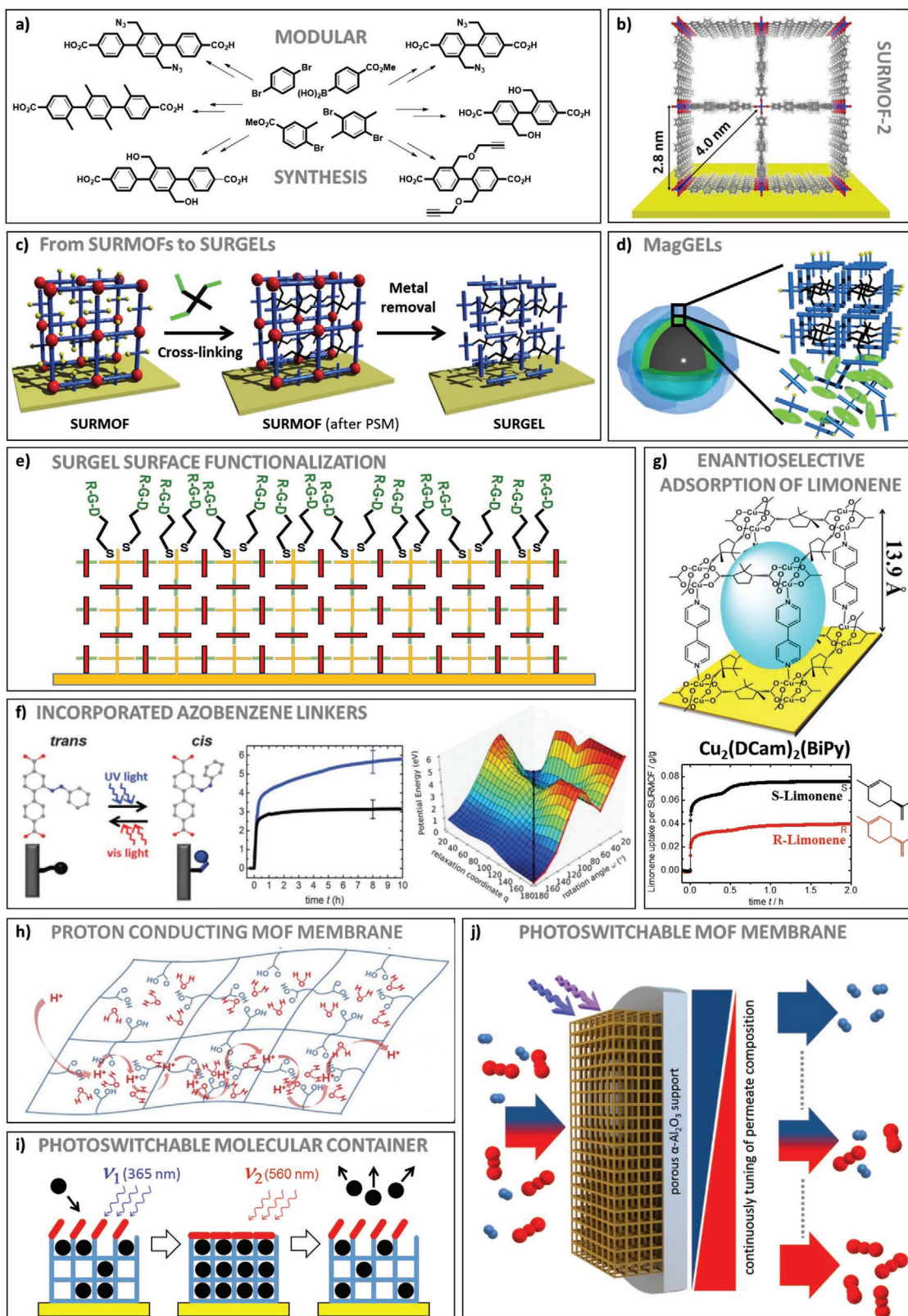


Figure 4. Organic chemistry for porous networks/research overview. a) Modular synthesis of functionalized ditopic organic linkers.^[63] b) Proposed structure of SURMOF-2. Reproduced with permission.^[65] Copyright 2012, Springer Nature. c) Schematic representation of the SURGELS' formation: before and after cross-linking, and after metal nodes removal. Adapted with permission.^[66] Copyright 2014, American Chemical Society. d) MagGEL capsule. Adapted with permission.^[68] Copyright 2015, American Chemical Society. e) Surface-modified SURGEL via thiol-ene click photoreaction.

functional organic linkers for the fabrication of porous networks. In this context, SML recently described a straightforward and efficient synthetic strategy for the preparation of linear ditopic functionalized organic linkers (Figure 4a).^[63] A modular library of diverse biphenyl, terphenyl, and higher linear linkers, based on Pd-catalyzed cross-coupling reactions, was investigated. In addition to serve as useful molecular bricks in the construction of different types of porous MOFs, the linkers exhibit functional side-groups—such as azide or alkyne moieties—suitable for postsynthetic modifications (PSM).^[64] Recently, it was demonstrated that monolithic MOF multilayers can be grown on a surface in a controlled way, using a step-by-step sequential procedure called liquid-phase epitaxy (LPE). These surface-supported metal–organic frameworks (SURMOFs) are grown layer by layer in a stepwise building block deposition process, allowing for a strict control of the film thickness and orientation. Importantly, the LPE process is accomplished by alternatively immersing the substrate into a solution of metal salt and an organic linker, allowing it to produce numerous hybrid and multi-heteroepitaxial SURMOFs. In 2012, the synthesis of a novel class of isorecticular surface-mounted metal–organic frameworks, namely SURMOF-2, from linear dicarboxylic acid linkers of different lengths and copper acetate using the liquid-phase epitaxy process was reported (Figure 4b).^[65] The obtained SURMOF-2 structures show high crystallinity and homogeneity, and their pore sizes could be finely tune by the use of linkers of the desired length; a channel size of $3 \times 3 \text{ nm}^2$ for the longest linker of five consecutive aromatic rings was obtained.

MOFs and SURMOFs are intrinsically unstable against water and the presence of cytotoxic metal ions, hence crippling their use in biological fields. To settle the problem, Tsotsalas et al. reported the fabrication of metal-free, 3D, highly porous, covalently bound polymer films of homogeneous thickness.^[66] These surface-grafted gels (SURGELS) combine the advantages of MOF materials, namely, the enormous flexibility and the large size of the maximum pore structures and, in addition, the possibility to grow them epitaxially on modified substrates, with those of covalently connected gel materials, namely, the absence of metal ions in the deposited material, a robust framework consisting of covalent bonds, and pronounced stability under biological conditions. Using linkers equipped with azide side groups, postsynthetic modifications of SURMOF frameworks via click chemistry become possible. The conversion of a SURMOF into a SURGEL is based on a covalent cross-linking of MOF linkers bearing two azide groups with a cross-linker bearing at least two alkyne groups via copper-free click chemistry, followed by the removal of metal clusters with ethylenediaminetetraacetic acid (EDTA) (Figure 4c). Such SURGELS can be loaded with bioactive compounds, applied as bioactive coatings and provide

a drug-release platform in in vitro cell culture studies. While these materials efficiently mediate the adhesion of cells on substrates, the process can be further enhanced by PSM of the surface, introducing at the top layer of the SURGEL molecules that exhibit a cell-specific recognition motif, such as the RGD (arginine-glycine-aspartic acid) amino-acid sequence (Figure 4e).^[67] Additionally, for bioapplications, the synthesis of hierarchically structured metal–organic framework multishells around magnetic core particles (MagMOFs) via layer-by-layer synthesis was reported.^[68] The sequential deposition method, combined with the SURGELS' approach, was used to create controlled release capsules (MagGELS), in which the inner and outer shells serves as a reservoir and a membrane, respectively, after post-synthetic modification (PSM) of the MOF structure into a SURGEL (Figure 4d). These capsules enable the controlled pH-dependent release of loaded dye molecules. Highly ordered proton-conducting polymer films starting from monolithic, crystalline MOF thin films were also reported.^[69] SURGELS, obtained by crosslinking the MOF thin films and subsequent metal removal, exhibit a long-range order and thus provide well-defined paths of hopping sites with a uniform distribution of distances (Figure 4h). Due to cross-linking, these SURGELS were found to exhibit superior proton conductivity and water stability, compared to conventional ion-conductive polymers.

Chiral materials offer great potential in enantioselective separation of chiral molecules, i.e., enantiomer separation, yet the design of materials that combine chirality and porosity in the same framework is tremendous challenging. Gu et al. investigated the influence of the pore size of chiral MOFs on the enantioselective adsorption of (*R*)- and (*S*)-limonene (Figure 4g).^[70] Three isorecticular chiral MOFs with the same chiral layer linker (*p*-camphoric acid), but different length of pillar linkers were prepared, and uptake experiments were monitored. The study clearly demonstrated that not only the stereogenic center, but also the pore size has to be adjusted to reach highest enantioselectivities in chiral nanoporous materials.

Another particularly attractive strategy for the fabrication of functional, smart materials consists in the incorporation of photoactive compounds into (SUR)MOFs. Integrated into the structure of such networks, photoswitchable molecules (e.g., azobenzene) enable the switching of physical and/or chemical properties in a fully contact-free controlled way. This was accomplished by the use of azobenzene-functionalized organic linkers for the synthesis of pillared-layer crystalline MOFs, enabling a precise understanding of light-induced, reversible molecular motion. Wang et al. demonstrated^[71] that based on both theoretical (density functional theory (DFT) calculation) and experimental (UV–vis spectroscopy/molecular uptake measurements) data such azobenzene-containing MOFs allow for the switching of azobenzene from *cis* to *trans* conformation in solid state. Such

Adapted with permission.^[67] Copyright 2016, Wiley-VCH. f) Structure of the azobenzene-containing linker (left), QCM uptake experiments without (black) and after (blue) UV irradiation (middle), calculated ground-state potential energy during the rotational isomerization of the azobenzene side group (right). Reproduced with permission.^[71] Copyright 2015, PCCP Owner Societies. Published by the Royal Society of Chemistry. g) Schematic structure of homochiral SURMOF (top), uptakes of (*S*)-limonene and (*R*)-limonene relative to the SURMOF mass measured by QCM (bottom). Reproduced with permission.^[70] Copyright 2015, The Royal Society of Chemistry. h) Schematic illustration of the highly organized polymer network in the SURGELS. Reproduced with permission.^[69] Copyright 2018, Wiley-VCH. i) Optically triggered uptake and release of guest molecule from two-component SURMOFs. Reproduced with permission.^[72] Copyright 2014, American Chemical Society. j) Tunable, remote-controllable molecular selectivity by a photoswitchable MOF membrane. Reproduced with permission.^[73] Copyright 2016, Nature Publishing Group.

photoswitchable SURMOFs can also be used as drug-release smart materials; respectively, Heinke et al. realized a two-component system with a separate storage region (a reservoir containing the molecules to be released) and a switching unit (stimulated with an optical signal) (Figure 4i)^[72] by installing vertical compositional gradients via liquid-phase epitaxy. After loading the porous coating with guest molecules, the release of the guest molecule, which is initiated by irradiation with visible light, was monitored by quartz crystal microbalance (QCM).

The potential use of SURMOFs as efficient separation membranes was also demonstrated.^[73,74] Explicitly, the azobenzene photoisomerization from *trans* to *cis* configuration and vice versa (stimulated with ultraviolet or visible light) resulted in a substantial modification of the membrane permeability and separation factor. The precise control of the *cis:trans* azobenzene ratio by controlled irradiation times and simultaneous irradiation with light enabled the continuous tuning of the separation and a continuous dynamic adjustment of the permeate flux (Figure 4j).

3. Conclusion and Outlook

The SML at KIT provides a platform for synthesis of smart and often bioinspired materials, and offers the advantage of implementing structures into defined shapes or thin films at all length scales. The strong interdisciplinary approach, combining polymer chemistry, organic chemistry, and materials sciences, establishes a comprehensive soft matter research environment allowing for the development of materials that are crucial for future areas such as (nano-)biomedicine or soft robotics. The use of externally triggered smart materials in applications of autonomous systems is crucial. In order to achieve this, we envision collaborations with other SMLs around the world that possess complementary expertise. The choice of chemistry has a considerable impact on the polymer synthesis as well as the chemical (post-)modification, which influences the structure–property relationship on nano- to microscale range. Further, the translation into a collective interaction requires a deeper knowledge in the area of physics and informatics. Our strong expertise in chemistry and polymer and material sciences contributes to research focused on applications in a collaborative space. Expanding the expertise by collaborations with other SMLs worldwide will lead to a better understanding of principles and processes leading to the implementation of a more complex constructs. Therefore, we reach out for a strong spirit of future collaborations.

Supporting Information

Supporting Information is available from the Wiley Online Library or from the author.

Acknowledgements

S.G., M.W., and H.M. contributed equally to this work. The authors acknowledge continued support from the Karlsruhe Institute of Technology (KIT) in the context of the Helmholtz BioInterfaces in Technology and Medicine (BIFTM) and Science and

Technology of Nanosystems (STN) programs as well as from the Sonderforschungsbereich (SFB1176) funded by the German Research Council (DFG). The authors also acknowledge the scientific contribution of the current and alumni members of SML, particularly B. Huber.

Conflict of Interest

The authors declare no conflict of interest.

Keywords

materials science, organic synthesis, polymer chemistry, soft matter

Received: September 30, 2018

Revised: October 24, 2018

Published online: February 10, 2019

- [1] A. V. Srinivasan, G. K. Haritos, F. L. Hedberg, *Appl. Mech. Rev.* **1991**, *44*, 463.
- [2] D. G. Castner, *Nature* **2003**, *422*, 129.
- [3] W. L. Murphy, T. C. McDevitt, A. J. Engler, *Nat. Mater.* **2014**, *13*, 547.
- [4] G. M. Bond, R. H. Richman, W. P. McNaughton, *J. Mater. Eng. Perform.* **1995**, *4*, 334.
- [5] J. F. V. Vincent, *Proc. Inst. Mech. Eng., Part H* **2009**, *223*, 919.
- [6] B. Bhushan, *Philos. Trans. R. Soc., A* **2009**, *367*, 1445.
- [7] R. Eisner, *The Scientist* **1991**, *July*, 14.
- [8] List of Soft Matter Laboratories, <http://www.ibg.kit.edu/ibg3/59.php> (accessed: October 2018).
- [9] T. Zincke, H. Günther, *Justus Liebig Ann. Chem.* **1893**, *272*, 243.
- [10] H. Sustmann, J. S. Clovis, A. Eckellz, R. Huisgen, *Chem. Ber.* **1967**, *100*, 1802.
- [11] S. Ulrich, D. Boturyn, A. Marra, O. Renaudet, P. Dumy, *Chem. - Eur. J.* **2014**, *20*, 34.
- [12] J. Collins, Z. Xiao, M. Mullner, L. A. Connal, *Polym. Chem.* **2016**, *7*, 3812.
- [13] T. Pauloehrl, G. Delaittre, M. Bruns, M. Meißler, H. G. Börner, A. M. Greiner, M. Bastmeyer, C. Barner-Kowollik, *Angew. Chem., Int. Ed.* **2012**, *51*, 9181.
- [14] G. Kaur, G. Singh, J. Singh, *Mater. Today Chem.* **2018**, *8*, 56.
- [15] T. Pauloehrl, G. Delaittre, V. Winkler, A. Welle, M. Bruns, H. G. Börner, A. M. Greiner, M. Bastmeyer, C. Barner-Kowollik, *Angew. Chem., Int. Ed.* **2012**, *51*, 1071.
- [16] C. Rodríguez-Emmenegger, C. M. Preuss, B. Yameen, O. Pop-Georgievski, M. Bachmann, J. O. Mueller, M. Bruns, A. S. Goldmann, M. Bastmeyer, C. Barner-Kowollik, *Adv. Mater.* **2013**, *25*, 6123.
- [17] T. Pauloehrl, G. Delaittre, M. Bruns, M. Meißler, H. G. Börner, M. Bastmeyer, C. Barner-Kowollik, *Angew. Chem.* **2012**, *124*, 9316.
- [18] Y. Sugawara, N. Jasinski, M. Kaupp, A. Welle, N. Zydziak, E. Blasco, C. Barner-Kowollik, *Chem. Commun.* **2015**, *51*, 13000.
- [19] J. Wang, W. Zhang, W. Song, Y. Wang, Z. Yu, J. Li, M. Wu, L. Wang, J. Zang, Q. Lin, *J. Am. Chem. Soc.* **2010**, *132*, 14812.
- [20] E. Blasco, M. Pinol, L. Oriol, B. V. K. J. Schmidt, A. Welle, V. Trouillet, M. Bruns, C. Barner-Kowollik, *Adv. Funct. Mater.* **2013**, *23*, 4011.
- [21] P. Lederhose, N. L. Haworth, K. Thomas, S. E. Bottle, M. L. Coote, C. Barner-Kowollik, J. P. Blinco, *J. Org. Chem.* **2015**, *80*, 8009.
- [22] D. Estupiñán, T. Gegenhuber, J. P. Blinco, C. Barner-Kowollik, L. Barner, *ACS Macro Lett.* **2017**, *6*, 229.
- [23] J. T. Offenloch, J. Willenbacher, P. Tzvetkova, C. Heiler, H. Mutlu, C. Barner-Kowollik, *Chem. Commun.* **2017**, *53*, 775.

- [24] D. Estupiñán, C. Barner-Kowollik, L. Barner, *Angew. Chem., Int. Ed.* **2018**, *57*, 5925.
- [25] H. Woehlke, J. Steinkoenig, C. Lang, L. Michalek, V. Trouillet, P. Krolla, A. S. Goldmann, L. Barner, J. P. Blinco, C. Barner-Kowollik, K. E. Fairfull-Smith, *Langmuir* **2018**, *34*, 3264.
- [26] H. Mutlu, C. W. Schmitt, N. Jasinski, H. Woehlke, K. Fairfull-Smith, J. P. Blinco, C. Barner-Kowollik, *Polym. Chem.* **2017**, *8*, 6199.
- [27] T. S. Fischer, S. Spann, Q. An, B. Luy, M. Tsotsalas, J. P. Blinco, H. Mutlu, C. Barner-Kowollik, *Chem. Sci.* **2018**, *9*, 4696.
- [28] R. Bogue, *Assem. Autom.* **2014**, *34*, 3.
- [29] P. Theato, B. S. Sumerlin, R. K. O'Reilly, T. H. Epps III, *Chem. Soc. Rev.* **2013**, *42*, 7055.
- [30] M. Wei, Y. Gao, X. Li, M. J. Serpe, *Polym. Chem.* **2017**, *8*, 127.
- [31] S. Harm-Jan, P. Leon, *J. Manuf. Technol. Manage.* **2016**, *27*, 990.
- [32] M. M. Zieger, P. Müller, E. Blasco, C. Petit, V. Hahn, L. Michalek, H. Mutlu, M. Wegener, C. Barner-Kowollik, *Adv. Funct. Mater.* **2018**, *28*, 1801405.
- [33] M. A. C. Stuart, W. T. S. Huck, J. Genzer, M. Müller, C. Ober, M. Stamm, G. B. Sukhorukov, I. Szleifer, V. V. Tsukruk, M. Urban, F. Winnik, S. Zauscher, I. Luzinov, S. Minko, *Nat. Mater.* **2010**, *9*, 101.
- [34] L. Montero de Espinosa, W. Meesorn, D. Moatsou, C. Weder, *Chem. Rev.* **2017**, *117*, 12851.
- [35] F. Ilievski, A. D. Mazzeo, R. F. Shepherd, X. Chen, G. M. Whitesides, *Angew. Chem.* **2011**, *123*, 1930.
- [36] S. Palagi, P. Fischer, *Nat. Rev. Mater.* **2018**, *3*, 113.
- [37] J.-K. Chen, C.-J. Chang, *Materials* **2014**, *7*, 805.
- [38] C. J. Brown, A. C. Farthing, *Nature* **1949**, *164*, 915.
- [39] D. J. Cram, H. Steinberg, *J. Am. Chem. Soc.* **1951**, *73*, 5691.
- [40] Z. Hassan, E. Spuling, D. M. Knoll, J. Lahann, S. Bräse, *Chem. Soc. Rev.* **2018**, *47*, 6947.
- [41] H.-Y. Chen, J. Lahann, *Langmuir* **2011**, *27*, 34.
- [42] W. E. Tenhaeff, K. K. Gleason, *Adv. Funct. Mater.* **2008**, *18*, 979.
- [43] H. G. Gilch, W. L. Wheelwright, *J. Polym. Sci., Part A-1: Polym. Chem.* **1966**, *4*, 1337.
- [44] H.-Y. Chen, J. Lahann, *Adv. Mater.* **2007**, *19*, 3801.
- [45] M. Koenig, R. Kumar, C. Hussal, V. Trouillet, L. Barner, J. Lahann, *Macromol. Chem. Phys.* **2017**, *218*, 1600521.
- [46] F. Bally-Le Gall, C. Hussal, J. Kramer, K. Cheng, R. Kumar, T. Eyster, A. Baek, V. Trouillet, M. Nieger, S. Bräse, J. Lahann, *Chem. - Eur. J.* **2017**, *23*, 13342.
- [47] L. del Mercato, P. Rivera-Gil, A. Z. Abbasi, M. Ochs, C. Ganas, I. Zins, C. Sönnichsen, W. J. Parak, *Nanoscale* **2010**, *2*, 458.
- [48] H. U. Kim, D. G. Choi, Y. H. Roh, M. S. Shim, K. W. Bong, *Small* **2016**, *12*, 3463.
- [49] J. Lahann, *Small* **2011**, *7*, 1149.
- [50] A. C. Misra, S. Bhaskar, N. Clay, J. Lahann, *Adv. Mater.* **2012**, *24*, 3850.
- [51] J. H. Jordahl, S. Ramcharan, J. V. Gregory, J. Lahann, *Macromol. Rapid Commun.* **2017**, *38*, 1600437.
- [52] M. Gil, S. Moon, J. Yoon, S. Rhamani, J.-W. Shin, K. J. Lee, J. Lahann, *Adv. Sci.* **2018**, *5*, 1800024.
- [53] A. Sitt, J. Soukupova, D. Miller, D. Verdi, R. Zboril, H. Hess, J. Lahann, *Small* **2016**, *12*, 1432.
- [54] a) E. Sokolovskaya, S. Rahmani, A. C. Misra, S. Braese, J. Lahann, *ACS Appl. Mater. Interfaces* **2015**, *7*, 9744; b) E. Sokolovskaya, J. Yoon, A. C. Misra, S. Bräse, J. Lahann, *Macromol. Rapid Commun.* **2013**, *34*, 1554.
- [55] K. J. Lee, J. Yoon, S. Rahmani, S. Hwang, S. Bhaskar, S. Mitragotri, J. Lahann, *Proc. Natl. Acad. Sci. USA* **2012**, *109*, 16057.
- [56] J. Yoon, T. W. Eyster, A. C. Misra, J. Lahann, *Adv. Mater.* **2015**, *27*, 4509.
- [57] N. Stock, S. Biswas, *Chem. Rev.* **2012**, *112*, 933.
- [58] Y. Cheng, A. Kondo, H. Noguchi, H. Kajiro, K. Urita, T. Ohba, K. Kaneko, H. Kanoh, *Langmuir* **2009**, *25*, 4510.
- [59] a) J. L. Rowsell, E. C. Spencer, J. Eckert, J. A. Howard, O. M. Yaghi, *Science* **2005**, *309*, 1350; b) S. Bourrelly, P. L. Llewellyn, C. Serre, F. Millange, T. Loiseau, G. Férey, *J. Am. Chem. Soc.* **2005**, *127*, 13519.
- [60] J. Kim, S.-N. Kim, H.-G. Jang, G. Seo, W.-S. Ahn, *Appl. Catal., A* **2013**, *453*, 175.
- [61] I. Stassen, N. Burtch, A. Talin, P. Falcaro, M. Allendorf, R. Ameloot, *Chem. Soc. Rev.* **2017**, *46*, 3185.
- [62] R. C. Huxford, J. Della Rocca, W. Lin, *Curr. Opin. Chem. Biol.* **2010**, *14*, 262.
- [63] S. Grosjean, Z. Hassan, C. Wöll, S. Bräse, *Eur. J. Org. Chem.* **2018**, <https://doi.org/10.1002/ejoc.201801232>.
- [64] M. Gotthardt, S. Grosjean, T. Brunner, J. Kotzel, A. Gänzler, S. Wolf, S. Bräse, W. Kleist, *Dalton Trans* **2015**, *44*, 16802.
- [65] J. Liu, B. Lukose, O. Shekha, H. K. Arslan, P. Weidler, H. Gliemann, S. Bräse, S. Grosjean, A. Godt, X. Feng, K. Müllen, I.-B. Magdau, T. Heine, C. Wöll, *Sci. Rep.* **2012**, *2*, 921.
- [66] M. Tsotsalas, J. Liu, B. Tettmann, S. Grosjean, A. Shahnas, Z. Wang, C. Azucena, M. Addicoat, T. Heine, J. Lahann, J. Overhage, S. Bräse, H. Gliemann, C. Wöll, *J. Am. Chem. Soc.* **2014**, *136*, 8.
- [67] S. Schmitt, J. Hümmer, S. Kraus, A. Welle, S. Grosjean, M. Hanke-Roos, A. Rosenhahn, S. Bräse, C. Wöll, C. Lee-Thedieck, M. Tsotsalas, *Adv. Funct. Mater.* **2016**, *26*, 8455.
- [68] S. Schmitt, M. Silvestre, M. Tsotsalas, A.-L. Winkler, A. Shahnas, S. Grosjean, F. Laye, H. Gliemann, J. Lahann, S. Bräse, M. Franzreb, C. Wöll, *ACS Nano* **2015**, *9*, 4219.
- [69] Z. Wang, C. Liang, H. Tang, S. Grosjean, A. Shahnas, J. Lahann, S. Bräse, C. Wöll, *Macromol. Rapid Commun.* **2018**, *39*, 1700676.
- [70] Z.-G. Gu, S. Grosjean, S. Bräse, C. Wöll, L. Heinke, *Chem. Commun.* **2015**, *51*, 8998.
- [71] Z. Wang, L. Heinke, J. Jelic, M. Cakici, M. Dommaschk, R. J. Maurer, H. Oberhofer, S. Grosjean, R. Herges, S. Bräse, K. Reuter, C. Wöll, *Phys. Chem. Chem. Phys.* **2015**, *17*, 14582.
- [72] L. Heinke, M. Cakici, M. Dommaschk, S. Grosjean, R. Herges, S. Bräse, C. Wöll, *ACS Nano* **2014**, *8*, 1463.
- [73] Z. Wang, A. Knebel, S. Grosjean, D. Wagner, S. Bräse, C. Wöll, J. Caro, L. Heinke, *Nat. Commun.* **2016**, *7*, 13872.
- [74] J. Caro, A. Knebel, L. Heinke, S. Grosjean, C. Wöll, Z. Wang, S. Bräse, *Eur. Pat. Appl. EP3305392*, **2018**.